THE JOURNAL OF PHYSICAL CHEMISTRY C
A JOURNAL OF THE AMERICAN CHEMICAL SOCIETY

pubs.acs.org/JPCC Article

Structure−Optical Property Relationship of Carbon Dots with Molecular-like Blue-Emitting Centers

Evgeny V. Kundelev,* Evgeny D. Strievich, Nikita V. Tepliakov, Anastasiia D. Murkina, Aliaksei Yu. Dubavik, Elena V. Ushakova, Alexander V. Baranov, Anatoly V. Fedorov, Ivan D. Rukhlenko, and Andrey L. Rogach

Cite This: J. Phys. Chem. C 2022, 126, 18170−18176 Read Online

ACCESS | Metrics & More | Article Recommendations | Supporting Information

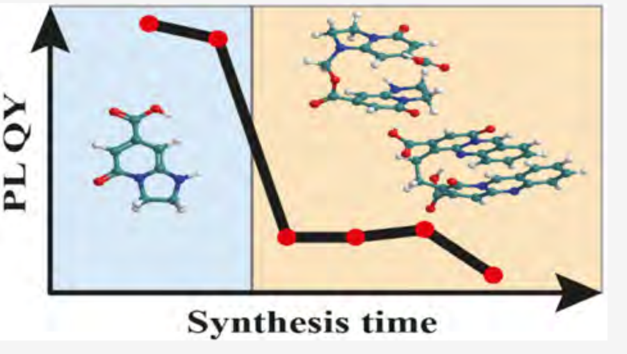

ABSTRACT: The determination of physical mechanisms governing photoluminescence (PL) of carbon dots (CDots) is required for fabrication of CDots with desired optical properties. Using the density functional theory, we comprehensively analyze how the changes in the structure of molecular centers during the synthesis of blue-emissive CDots affect their optical properties. Our calculations predict a pronounced red shift of the PL peak and a decrease in the PL intensity of CDots by up to 2 orders of magnitude when the monomer-like molecular centers are replaced by the covalent or noncovalent dimers of the molecular fluorophore IPCA (5-oxo-1,2,3,5-tetrahydroimidazo-[1,2-α]pyridine-7-carboxylic acid). The predicted red shift of the PL peak can be significantly reduced by shortening the length of the conjugated π-system in the IPCA-like molecular centers caused by presence of oxygen atoms, which can be achieved through substitution of nitrogen with oxygen atoms in the conjugated π-system. To verify our theoretical predictions, we varied the synthesis time of the blue-emissive CDots with the IPCA-like molecular centers made from citric acid and ethylenediamine. The PL intensity of these CDots is found to initially rise for the synthesis times between 1 and 2 h and then to dramatically decrease by a factor of 2 and remain almost constant for synthesis times of up to 6 h, with a weak PL peak appearing at longer wavelengths. These trends could be well reproduced by numerical simulations assuming they are caused by the structural changes in the blue-emissive IPCA-like molecular centers of the CDots. The revealed structure−function relationship of CDots with molecular-like centers can explain similar trends in the PL spectra of CDots obtained from other precursors.

■ INTRODUCTION

Carbon dots (CDots) have recently emerged as a promising carbon nanomaterial offering bright and tunable photoluminescence (PL).[1−5] The photophysics of the CDots' PL is still under intense scrutiny due to the complexity of the internal and surface structure of CDots as well as a variety of synthesis techniques and precursor materials.[6,7] It is generally accepted that the PL contributions from the core, surface states, and molecular centers are determined by the synthesis technique.[7−10] The core states originating from the sp^2-hybridized aromatic domains in CDots usually yield radiative transitions of the $\pi-\pi^*$ nature.[11−14] The surface states from the outer parts of the amorphous sp^3-hybridized matrix result in the $\pi-\pi^*$ and $n-\pi^*$ transitions, whose energy is reduced as compared to the core states.[15−18] CDots may also include different kinds of molecular-like luminescent centers, whose contribution to the PL signal typically decreases with raising the synthesis temperature.[19−24] As a consequence, molecular-like centers mostly determine the optical features of CDots which are synthesized at temperatures below 200 °C.[25,26]

Yang's group was the first to identify bright blue-emissive molecular centers of CDots in the form of IPCA (5-oxo-1,2,3,5-tetrahydroimidazo[1,2-α]pyridine-7-carboxylic acid) for samples synthesized at 190 °C using citric acid and ethylenediamine as precursors.[25] The synthesis of nitrogen−sulfur-co-doped CDots from citric acid and L-cysteine under similar conditions produced blue-emissive CDots with molecular centers in the form of TPCA (5-oxo-3,5-dihydro-2H-thiazalo[3,2-α]pyridine-7-carboxylic acid).[27] The limited number of constituting atoms in those molecular centers and their well-reported contributions to optical response of the CDots enable one to analyze the trends and patterns in the luminescence−structure relationship of the CDots using the

Received: August 18, 2022
Revised: October 3, 2022
Published: October 12, 2022

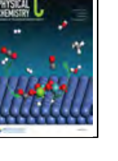

https://doi.org/10.1021/acs.jpcc.2c05926
J. Phys. Chem. C 2022, 126, 18170−18176

density functional theory (DFT). This analysis showed that the geometric configuration of the IPCA dimers strongly affects the PL intensity of CDots.[28] Langer et al. theoretically studied the impact of the molecular fluorophore IPCA on the excitation-independent PL of CDots.[29] It was shown that the interaction between the molecular centers within the CDots not only significantly reduces the PL intensity but also broadens and red-shifts their PL and absorption spectra.[30,31] It also became clear that even small changes in the structure of interacting molecular-like centers during the synthesis of CDots can substantially modify their optical response. Therefore, the investigation of possible structural changes of molecular-like centers and the formation of their derivatives during the synthesis of CDots is paramount for unrevealing the general trends and patterns in the optical spectra of CDots.

In this study, we first employ DFT calculations to analyze the impact of the formation of IPCA-like surface molecular centers and the changes in their structure with the synthesis time on the optical properties of CDots. We show that the increase in the conjugation length of the centers, achieved by the addition of additional rings, red-shifts the absorption and PL spectra of CDots. The same effect entails their covalent and noncovalent coupling, but with the decrease in the emission intensity. Substitution of nitrogen atoms by oxygen atoms in the conjugation system of the IPCA-like surface molecular centers is shown to blue-shift the optical spectra. To track the changes in the optical properties of blue-emissive CDots during their synthesis, we then synthesize CDots with the IPCA-like molecular centers from citric acid and ethylenediamine by varying the synthesis time from 1 to 6 h with a 1 h step. This is followed by the optical characterization of the CDots, which shows that the PL intensity increases with the synthesis time from 1 to 2 h and then steeply decreases by a factor of 2 and remains almost independent of the synthesis time of up to 6 h, while an extra PL peak appears at longer wavelengths. Numerical simulations make us conclude that the steep decline in the PL intensity and the additional PL peak can be associated with the structural changes in these CDots.

METHODS

Modeling of CDots' Spectra. The functional subunits of CDots were subjected to the ground-state geometry optimization within the DFT framework with the hybrid exchange-correlation density functional (B3LYP),[32] the empirical dispersion correction Grimme D4 (DFT-D4),[33] and the standard DZP Slater-type basis set.[34] The energies and oscillator strengths were calculated by using the TDDFT approach with the B3LYP functional, dispersion correction Grimme D4, and the DZP basis set. To calculate the energies and oscillator strengths of the electronic transitions in the PL spectra, we performed the geometry optimization of the excited state within the frame of the DFT/B3LYP-D4/DZP approach and the linear-response TDDFT/B3LYP-D4/DZP calculations for radiative transitions. The absorption and PL spectra were obtained for CDots dissolved in water, which was considered using the conductor-like screening model (COSMO).[35] All calculations were performed using the Amsterdam density functional (ADF) package.[36,37]

Synthesis of CDots. CDots were synthesized according to the standard hydrothermal synthetic protocol[25]. 1.0507 g of citric acid and 335 μL of ethylenediamine (water solution of 0.899 g/mL concentration) were dissolved in 10 mL of distilled water and transferred into Teflon autoclaves. The autoclaves were placed in a muffle furnace and held at 190 °C for 1, 2, 3, 4, 5, and 6 h. After the cooling of autoclaves to room temperature, the obtained CDot solutions were subjected to dialysis to remove any byproducts formed during the synthesis.

Characterization. Absorption spectra of CDots were measured on a Shimadzu UV-3600 spectrophotometer, and PL spectra were measured on a Cary Eclipse spectrophotometer. The PL QY of CDots was estimated by the reference point method as

$$\varphi = \varphi_R (I/I_R)(D_R/D)(n/n_R)^2$$

where φ is the PL QY, I is the integrated emission intensity, n is the refractive index of the solvent (water), and D is the optical density. The subscript "R" refers to the reference solution of Rhodamine 6G (chosen as the standard with a PL QY of 0.95), which was dissolved in ethanol.

RESULTS AND DISCUSSION

The IPCA molecule and its derivatives have been reported to determine the optical response of blue-emissive CDots obtained by the hydrothermal synthesis from citric acid and ethylenediamine.[25] We thus analyzed the optical response of CDots with different IPCA-like molecular centers on the surface using the quantum-chemical DFT calculations. Three types of surface molecular centers are considered: the free centers (F), the interaction between which is negligible; the loosely bound centers (L), which are coupled by the weak noncovalent binding forces; and the tightly bound centers (T) coupled by the stronger, covalent binding forces. The tightly bound centers can be connected by two, three, or four carbon linkers. We assumed that the surface molecular centers are attached to the CDot's core by flexible aliphatic linkers, which do not affect the optical response of the CDot. The surface molecular centers are thus modeled as disconnected from the core free-standing subunits (Figure 1a). Similarly, a pair of weakly coupled centers is approximated by a free-standing noncovalently bound dimer (Figure 1b), and the tightly coupled centers are modeled as isolated covalent dimers without aliphatic linkers (Figure 1c).

We assume that the free-standing subunits comprise IPCA molecules and their derivatives, as it was established for the CDots synthesized by the hydrothermal method from citric acid and ethylenediamine.[25] The simplest subunits are represented by an IPCA molecule composed of fused six- and five-membered rings (subunit F0) and its derivatives with two (F1) or three (F2) six-membered conjugated rings or with a five-membered ring (F3) where a nitrogen atom is substituted by an oxygen atom (Figure 1a). Subunits F1, F2, and F3 can be obtained experimentally by replacing ethylenediamine with 1,3-diaminopropane, 2-aminobenzylomine, and ethanolamine, respectively. The noncovalent (L0, L1, L2, and L3) and covalent (T0, T1, T2, and T3) subunits are dimers made up from subunits F0, F1, F2, and F3 (Figures 1b and 1c). The covalent subunits are bound by one (T0), two (T2 and T3), and five carbon linkers (T1), as shown in Figure 1c. This binding is assumed to occur via nitrogen (T0) and oxygen (T1) atoms, benzene rings (T2), or a benzene ring and a five-membered ring (T3). Considering those three types of the IPCA-based subunits (F, L and T) allows us to capture the general trends and patterns in the PL of real blue-emissive CDots with various kinds of surface molecular centers obtained

https://doi.org/10.1021/acs.jpcc.2c05926
J. Phys. Chem. C 2022, 126, 18170−18176

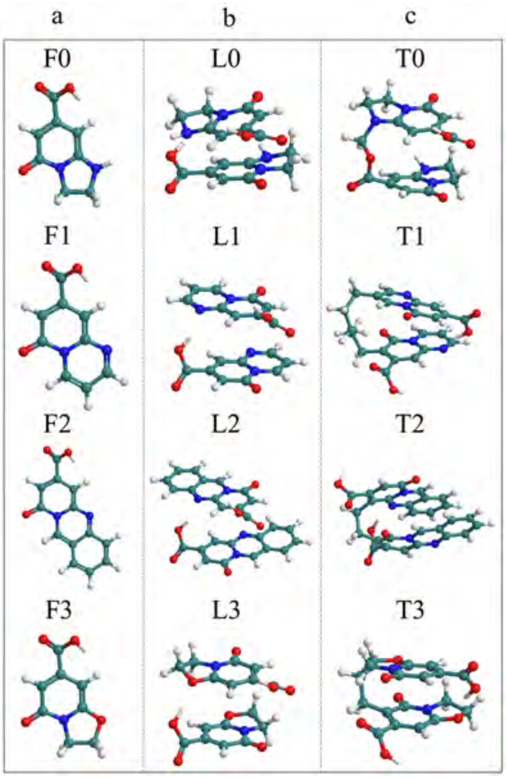

Figure 1. (a) Free (F), (b) loosely bound (L), and (c) tightly bound (T) surface subunits of CDots. The free centers are represented by the IPCA molecule (subunit F0) and its derivatives with two six-membered rings (F1), three six-membered rings (F2), and a five-membered ring (F3) with one nitrogen atom substituted by an oxygen atom. The loosely and tightly bound centers are noncovalent (L0, L1, L2, and L3) and covalent (T0, T1, T2, and T3) dimers of the IPCA molecule (F0) and its derivatives (F1, F2, and F3).

by hydrothermal synthesis from the citric acid and ethylenediamine precursors.

Figure 2a−d shows the absorption spectra of the four IPCA-based surface subunits, calculated using the time-dependent DFT approach as discussed in the Methods section. The subunit F0 (IPCA molecule) has three distinct absorption bands centered at 200, 231, and 363 nm. The position of the long-wavelength band is in good agreement with the experimental value reported for IPCA, whereas the positions of the other two bands differ by 150 and 119 nm, respectively.[25] The absorption parameters of the IPCA molecule are given in Tables S1 and S2.

The increase in the number of the conjugated π-electrons with the replacement of the five-membered ring in subunit F0 by one (F1) or two (F2) six-membered rings red-shifts the absorption bands (Figures 2b and 2c). The low-energy absorption bands of subunits F1 and F2 are red-shifted by 27 and 176 nm relative to the corresponding band F0 and are centered at 390 and 539 nm, respectively. The decrease in the number of the delocalized π-electrons in the conjugated system of subunit F3 with the substitution of a nitrogen atom within the five-membered ring by an oxygen atom accounts for the blue shift of the absorption bands. Therefore, the low-energy absorption peak has a blue shift of 20 nm relative to the similar peak of F0, and it is centered at 343 nm (Figure 2d).

The weak interaction between IPCA molecules within a noncovalent subunit L0 creates additional absorption transitions, changes oscillator strengths of the absorption bands, and shifts the bands to longer wavelengths (Figure 3a). In particular, the low-energy band red-shifts by 57 nm (to 420 nm) and significantly decreases in intensity as compared to the similar band of F0. The weak interaction between the monomers of the IPCA derivatives within subunits L1, L2, and L3 causes similar changes in their absorption spectra, red-shifting the long-wavelength absorption bands by 44, 103, and 29 nm to 434, 642, and 372 nm, respectively (Figure 3b,c and Table 1). The tight coupling via carbon linkers within the covalent subunits T0, T1, T2, and T3 leads to further redistribution of the absorption efficiency (Figure 3e−h). The wavelengths of the low-energy absorption bands increase by 27, 31, 110, and 4 nm relative to the similar bands of the free subunits and become 390, 421, 649, and 347 nm, respectively.

To calculate the PL spectra of CDots with surface emission centers, we successively performed the excited-state geometry optimization using the DFT approach and the linear-response TDDFT calculations of the first excited state of the considered subunits. For subunit F0, our simulations predict a 472 nm PL peak with the oscillator strength of 0.167 (Figure 2e and Table 1). The peak's position is close to the experimental value of 442 nm reported for an aqueous solution of CDots[25] and also correlates well with the available numerical data.[28] A 109 nm Stokes shift of the peak (Table 1), predicted by our simulations, is also close to the experimental and theoretical values of 91 and 73 nm reported for the IPCA molecule.[25,28]

The PL spectra of the subunits based on the monomers of the IPCA-derived molecules are presented in Figure 2e−h. The

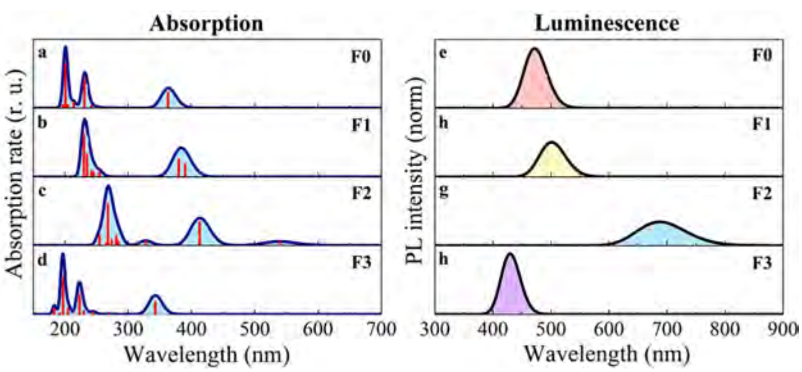

Figure 2. Absorption and PL spectra of free surface subunits shown in Figure 1a. Vertical red sticks are used to illustrate the oscillator strengths of individual electronic transitions. Each transition is represented by Gaussian line shape with a full width at half-maximum (FWHM) of 0.15 eV.

https://doi.org/10.1021/acs.jpcc.2c05926
J. Phys. Chem. C 2022, 126, 18170−18176

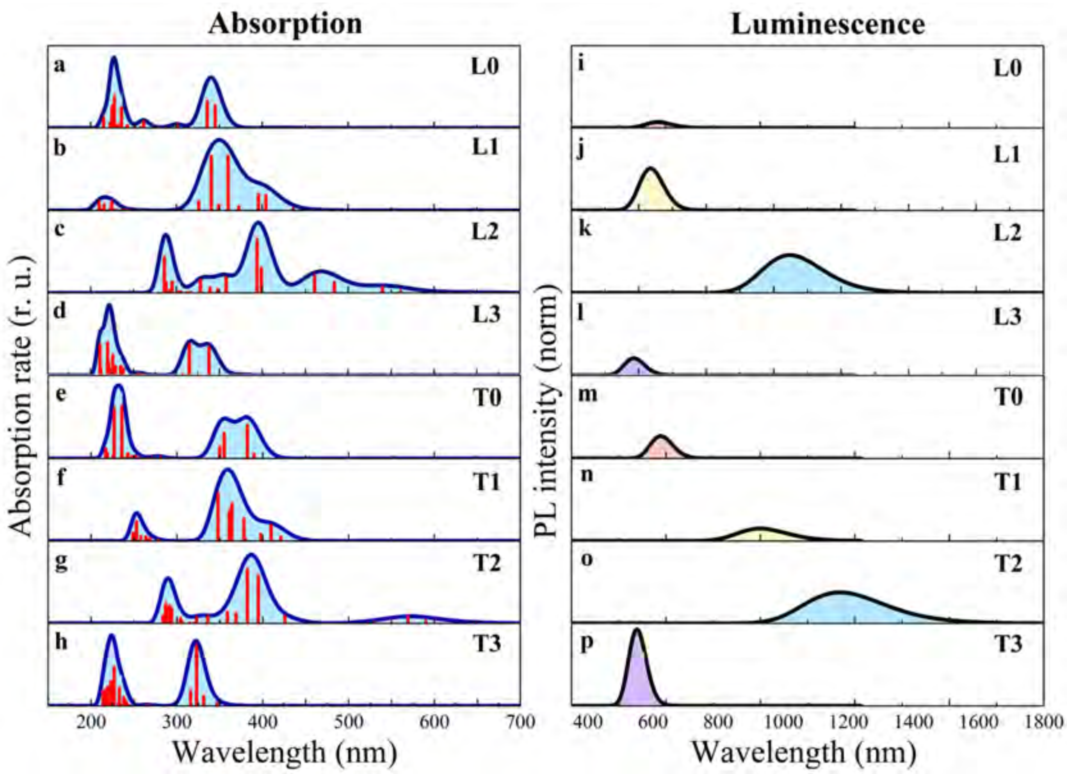

Figure 3. Absorption and PL spectra of noncovalent and covalent surface subunits shown in Figure 1b,c. Vertical red sticks are used to illustrate the oscillator strengths of individual electronic transitions. Each transition is represented by Gaussian line shape with a FWHM of 0.15 eV.

Table 1. Wavelengths (λ) and Oscillator Strengths (f) of the Lowest-Energy Absorption and PL Transitions of the IPCA-like Subunits Shown in Figure 1[a]

subunit	λ_A (nm)	f_A	λ_{PL} (nm)	f_{PL}	$\lambda_{PL} - \lambda_A$ (nm)
F0	363	0.222	472	0.167	109
F1	390	0.186	501	0.097	111
F2	539	0.078	687	0.066	148
F3	343	0.211	430	0.170	87
L0	420	0.003	657	0.001	237
L1	434	0.008	635	0.010	201
L2	642	0.006	1020	0.009	378
L3	372	0.005	585	0.004	213
T0	390	0.026	624	0.006	234
T1	421	0.023	929	0.003	508
T2	649	0.005	1174	0.008	525
T3	347	0.015	551	0.019	204

[a]The last column provides the values of the Stokes shift between the PL and absorption maxima.

PL peaks are seen to red-shift with the number of the six-membered rings in the sequence F0, F1, and F2 and blue-shift with the replacement of the nitrogen atom in the five-membered ring (subunit F0) by an oxygen atom (F3). The PL peaks of subunits F1, F2, and F3 are centered at 501, 687, and 430 nm, respectively (Table 1). The red shift of the PL peaks is attributed to the increased number of delocalized π-electrons, whereas the blue shift is attributed to the decreased number of electrons in the conjugated π-system. The Stokes shift in the spectra of the subunits increases with the number of conjugated rings from 109 nm for the IPCA molecule (subunit F0) to 111 and 148 nm for subunits S1 and S2, respectively, and decreases to 87 nm with the replacement of the nitrogen atom in the five-membered ring (subunit F0) by an oxygen atom (F3). The predicted Stokes shifts are in accord with those observed for CDots obtained from citric acid and ethylenediamine.[25]

The PL spectra of the interacting subunits are shown in Figure 3i−p. The PL peaks of the noncovalently bound subunits L0, L1, L2, and L3 are at 657, 635, 1020, and 585 nm, respectively. The PL rates within the respective bands are reduced about 10-fold for subunits L1 and L2 and about 100-fold for subunits L0 and L3 as compared to free subunits F1, F2, F0, and F3. The calculated Stokes shift varies from 201 and 213 nm for subunits L1 and L3 to 237 and 378 nm for subunits L0 and L2, respectively (Table 1). The PL peaks of the covalently bound subunits T0, T1, T2, and T3 are centered at 624, 929, 1174, and 551 nm, respectively. Similar to the noncovalently bound subunits, covalent linking weakens PL by a factor of 100 for subunit T0 and by a factor of 10 for subunits T1, T2, and T3. The Stokes shifts are 234 and 204 nm for the covalent subunits T0 and T3 (close to the shifts for noncovalent subunits) and 508 and 525 nm for subunits T1 and T2. Notably, theoretical Stokes shifts from 200 to 500 nm for the interacting subunits are much larger than the experimentally obtained values.[19] This is due to the considerable change in the geometric configuration of the subunits upon their relaxation from the excited state to the ground state.[38]

Our simulations predict that the interaction among the IPCA-like surface emission centers can suppress the PL of the blue-emissive CDots. This is evidenced by the data in Table 1, which shows that the loose and tight bindings of the IPCA-like subunits reduce the oscillator strengths of the PL transitions by up to 2 orders of magnitude as compared to the free subunits. We hypothesize that this reduction would manifest itself in the

https://doi.org/10.1021/acs.jpcc.2c05926
J. Phys. Chem. C 2022, 126, 18170−18176

weakening of the CDots' luminescence upon the formation of the emission centers inside the CDots. The interaction among such centers strengthens with increasing the synthesis time, which explains the experimentally observed decrease in the PL QY of the blue-emissive CDots.[25,39]

To verify our hypothesis, a set of blue-emissive CDots was synthesized by the standard hydrothermal method from citric acid and ethylenediamine at 190 °C, as described in ref 26 and the Methods section. The CDots obtained for the synthesis times of 1 h, 2 h, etc. are denoted as 1h-CDots, 2h-CDots, etc. The absorption and PL spectra of the synthesized CDots are showed in Figure 4. The PL spectra are normalized by the

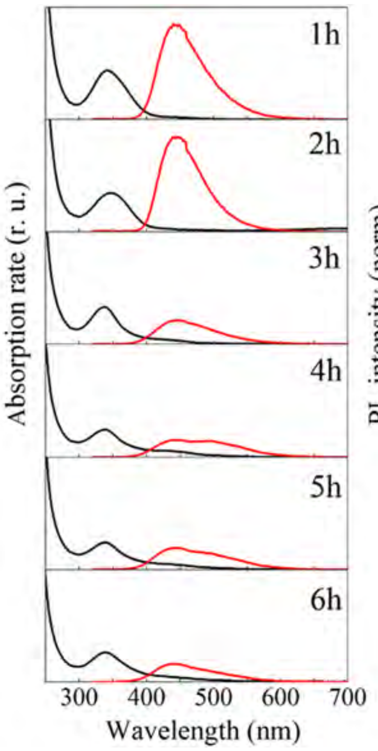

Figure 4. Absorption (black) and PL (red) spectra of CDots synthesized by the standard hydrothermal method from citric acid and ethylenediamine at 190 °C, where the synthesis time varied from 1 to 6 h. All PL spectra are normalized to the optical density at the excitation wavelength of 290 nm.

optical density at the excitation wavelength of 290 nm. 1h-CDots and 2h-CDots have characteristic absorption peaks at 341 and 345 nm, respectively, and a PL peak at 445 nm. The position and shape of the PL peak are close to those observed for blue-emissive CDots from citric acid and ethylenediamine under the same conditions.[25] These CDots contain emission centers, which were identified as the IPCA molecules with emission at 442 nm.

With the increase of the synthesis time, the position of the absorption band red-shifts from 341 nm for 1h-CDots to 345 nm for 2h-CDots and blue-shifts to 338 nm for the rest of the CDots samples. At the same time, the absorption band become narrower, and a broad shoulder appears between 400 and 500 nm. The PL intensity is the largest for 2h-CDots, 4 times smaller for 3h-CDots, and 5 times smaller for the rest of the CDots. The position of the main PL peak at 345 nm does not depend on the synthesis time, and a new PL peak appears at 495 nm for 4h-CDots and at 500 nm for 5h-CDots. The shifts of the absorption and PL peaks observed with the increase of the synthesis time are less pronounced than the shifts predicted theoretically, especially for subunits L2, T1, and T2. This discrepancy can be due to the predominant formation of molecular centers with a small conjugated π-system and centers doped with oxygen, resulting in the absorption and PL that are more typical for the subunits L0, L1, L3, T0, and T3.

Figure 5 shows that the PL QY decreases from a maximum value of 51% for 1h-CDots down to 18% for 6h-CDots, with a

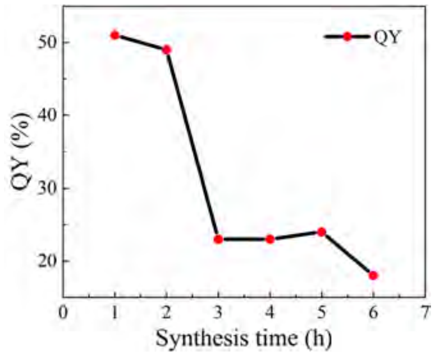

Figure 5. Peak PL QY (red circles) of CDots as functions of synthesis time.

rather strong drop from 49% to 23% after 3 h of synthesis. The drop in the PL QY of CDots with the synthesis time can be attributed to the transition from a molecular-like state to a carbonized structure of CDots.[25] This transition increases the possibility of stronger interaction between the emission centers, which according to our calculations significantly weakens the PL intensity of CDots. The experimentally observed decrease of the PL QY by a factor of 2.8 is also consistent with the results of our numerical simulations, which predict a 2-fold drop in the intensity. It should be noted that the theoretically predicted trends of the PL intensity do not consider nonradiative relaxation processes, which could reduce the PL intensity and further improve the agreement between the theory and experiment. The appearance of new PL peaks for 4h-CDots and 5h-CDots may be caused by the modification of the original emission centers or the formation of new ones with smaller PL intensity. The energy shifts in the experimental absorption and PL spectra of CDots are smaller than predicted shifts, which can be explained by the partial cancellation of the increase in the length of the conjugated π-systems and their coupling with each other due to the withdrawal of electrons from the conjugated π-systems with oxygen.

The observed PL weakening with the increase of synthesis time strongly correlates with increasing carbonization degree of CDots.[38] Krysmann et al. reported that the PL intensity of CDots decreases with the synthesis temperature, while the carbonization degree increases.[25,39] Correlations in the time and temperature dependencies of the PL QY and carbonization degree of CDots suggest that the main sources of bright PL in CDots predominantly arise at relatively low temperatures in the early stages of synthesis, which precede the formation of the carbogenic core. The formation of the CDots' luminescent centers at low temperatures resembles the synthesis of luminescent dyes under similar conditions, whereas the CDots' core is formed at higher temperatures.[26] The CDot's core has a graphite-like band structure, acting as a PL

https://doi.org/10.1021/acs.jpcc.2c05926
J. Phys. Chem. C 2022, 126, 18170−18176

quencher, and this effect becomes stronger with the carbonization degree of CDots. Therefore, by reducing the synthesis time and temperature, one can create brighter and less carbogenic CDots. Small polycyclic aromatic hydrocarbons or molecular centers and their aggregates on the CDot's surface determine the main features of the CDot's luminescence, whereas the carbogenic part of the CDot, with a periodic lattice-like pattern evidenced by HRTEM images,[19] would rather weaken the PL.

■ CONCLUSIONS

In summary, we have performed a comprehensive DFT/experimental analysis on how IPCA-like surface molecular centers and possible changes in their structure with synthesis time influences the optical properties of blue-emissive CDots. Our DFT calculations revealed the red shifts of the absorption and PL spectra of CDots due to the increased conjugation lengths of the IPCA-like centers caused by adding additional rings. The red shifts of the spectra were observed upon the covalent and noncovalent couplings of the surface molecular centers of CDots, yet with weakening of the emission intensity by 2 orders of magnitude. It was shown that the reduction in the number of the conjugated π-electrons due to the substitution of nitrogen atoms by oxygen atoms in the conjugation system of the IPCA-like surface molecular subunits leads to the blue shift of the optical spectra of CDots. The experimental study showed that the formation of bright blue-emissive centers occurs at an early stage of synthesis of CDots, namely within the first 1 or 2 h. The coupling and modification of these surface molecular centers then lead to a steep 2-fold decrease of the PL intensity (QY), which is also predicted by our calculations. Our study not only provides valuable insights into the structure−optical property relationship of CDots but also may be useful for developing novel synthetic pathways toward bright CDots.

■ ASSOCIATED CONTENT

Supporting Information

The Supporting Information is available free of charge at https://pubs.acs.org/doi/10.1021/acs.jpcc.2c05926.

Additional data on energies, oscillator strengths, and composition of electronic transitions in the IPCA-based surface subunits of CDots (PDF)

■ AUTHOR INFORMATION

Corresponding Author

Evgeny V. Kundelev − *Information Optical Technologies Center, ITMO University, St. Petersburg 197101, Russia;* orcid.org/0000-0002-7672-1790; Email: kundelev.evg@gmail.com

Authors

Evgeny D. Strievich − *Information Optical Technologies Center, ITMO University, St. Petersburg 197101, Russia*

Nikita V. Tepliakov − *Departments of Materials and Physics, Imperial College London, London SW7 2AZ, United Kingdom; Information Optical Technologies Center, ITMO University, St. Petersburg 197101, Russia*

Anastasiia D. Murkina − *Information Optical Technologies Center, ITMO University, St. Petersburg 197101, Russia*

Aliaksei Yu. Dubavik − *Information Optical Technologies Center, ITMO University, St. Petersburg 197101, Russia*

Elena V. Ushakova − *Information Optical Technologies Center, ITMO University, St. Petersburg 197101, Russia;* orcid.org/0000-0001-6841-6975

Alexander V. Baranov − *Information Optical Technologies Center, ITMO University, St. Petersburg 197101, Russia*

Anatoly V. Fedorov − *Information Optical Technologies Center, ITMO University, St. Petersburg 197101, Russia;* orcid.org/0000-0002-7395-0985

Ivan D. Rukhlenko − *Institute of Photonics and Optical Science (IPOS), School of Physics, The University of Sydney, Camperdown 2006 NSW, Australia; Information Optical Technologies Center, ITMO University, St. Petersburg 197101, Russia;* orcid.org/0000-0001-5585-4220

Andrey L. Rogach − *Department of Materials Science and Engineering, and Centre for Functional Photonics (CFP), City University of Hong Kong, Hong Kong SAR 999077, China;* orcid.org/0000-0002-8263-8141

Complete contact information is available at: https://pubs.acs.org/10.1021/acs.jpcc.2c05926

Notes

The authors declare no competing financial interest.

■ ACKNOWLEDGMENTS

This work was financially supported by the Russian Science Foundation (RSF22-13-00294) and by the Research Grant Council of Hong Kong S.A.R. (CityU 11306619). E.V.K. thanks the Ministry of Science and Higher Education of the Russian Federation for financial support through the Scholarship of the President of the Russian Federation for young scientists and graduate students (СП-1807.2022.1). N.V.T. acknowledges the President's PhD Scholarship of Imperial College London.

■ REFERENCES

(1) Xu, X.; Ray, R.; Gu, Y.; Ploehn, H. J.; Gearheart, L.; Raker, K.; Scrivens, W. A. Electrophoretic Analysis and Purification of Fluorescent Single-Walled Carbon Nanotube Fragments. *J. Am. Chem. Soc.* **2004**, *126*, 12736−12737.

(2) Baker, S. N.; Baker, G. A. Luminescent Carbon Nanodots: Emergent Nanolights. *Angew. Chem., Int. Ed.* **2010**, *49*, 6726−6744.

(3) Xiao, L.; Sun, H. Novel Properties and Applications of Carbon Nanodots. *Nanoscale Horiz.* **2018**, *3*, 565−597.

(4) Zhu, S.; Meng, Q.; Wang, L.; Zhang, J.; Song, Y.; Jin, H.; Zhang, K.; Sun, H.; Wang, H.; Yang, B. Highly Photoluminescent Carbon Dots for Multicolor Patterning, Sensors, and Bioimaging. *Angew. Chem., Int. Ed.* **2013**, *52*, 3953−3957.

(5) Yuan, F.; Wang, Z.; Li, X.; Li, Y.; Tan, Z.; Fan, L.; Yang, S. Bright Multicolor Bandgap Fluorescent Carbon Quantum Dots for Electroluminescent Light-Emitting Diodes. *Adv. Mater.* **2017**, *29*, 1604436.

(6) Xia, C.; Zhu, S.; Feng, T.; Yang, M.; Yang, B. Evolution and Synthesis of Carbon Dots: From Carbon Dots to Carbonized Polymer Dots. *Adv. Sci.* **2019**, *6*, 1901316.

(7) Langer, M.; Paloncýová, M.; Medved', M.; Pykal, M.; Nachtigallová, D.; Shi, B.; Aquino, A. J. A.; Lischka, H.; Otyepka, M. Progress and Challenges in Understanding of Photoluminescence Properties of Carbon Dots Based on Theoretical Computations. *Appl. Mater. Today* **2021**, *22*, 100924.

(8) Carbonaro, C. M.; Corpino, R.; Salis, M.; Mocci, F.; Thakkar, S. V.; Olla, C.; Ricci, P. C. On the Emission Properties of Carbon Dots: Reviewing Data and Discussing Models. *C* **2019**, *5*, 60.

(9) Tepliakov, N. V.; Kundelev, E. V.; Khavlyuk, P. D.; Xiong, Y.; Leonov, M. Y.; Zhu, W.; Baranov, A. V.; Fedorov, A. V.; Rogach, A. L.; Rukhlenko, I. D. Sp2-Sp3-Hybridized Atomic Domains Determine Optical Features of Carbon Dots. *ACS Nano* **2019**, *13*, 10737−10744.

(10) Yu, J.; Yong, X.; Tang, Z.; Yang, B.; Lu, S. Theoretical Understanding of Structure-Property Relationships in Luminescence of Carbon Dots. *J. Phys. Chem. Lett.* **2021**, *12*, 7671−7687.

(11) Kwon, W.; Lee, G.; Do, S.; Joo, T.; Rhee, S. W. Size-Controlled Soft-Template Synthesis of Carbon Nanodots toward Versatile Photoactive Materials. *Small* **2014**, *10*, 506−513.

(12) Sudolska, M.; Dubecky, M.; Sarkar, S.; Reckmeier, C. J.; Zboril, R.; Rogach, A. L.; Otyepka, M. Nature of Absorption Bands in Oxygen-Functionalized Graphitic Carbon Dots. *J. Phys. Chem. C* **2015**, *119*, 13369−13373.

(13) Yoon, H.; Chang, Y. H.; Song, S. H.; Lee, E. S.; Jin, S. H.; Park, C.; Lee, J.; Kim, B. H.; Kang, H. J.; Kim, Y. H.; et al. Intrinsic Photoluminescence Emission from Subdomained Graphene Quantum Dots. *Adv. Mater.* **2016**, *28*, 5255−5261.

(14) Sk, M. A.; Ananthanarayanan, A.; Huang, L.; Lim, K. H.; Chen, P. Revealing the Tunable Photoluminescence Properties of Graphene Quantum Dots. *J. Mater. Chem. C* **2014**, *2*, 6954−6960.

(15) Hu, S.; Tian, R.; Dong, Y.; Yang, J.; Liu, J.; Chang, Q. Modulation and Effects of Surface Groups on Photoluminescence and Photocatalytic Activity of Carbon Dots. *Nanoscale* **2013**, *5*, 11665−11671.

(16) Holá, K.; Sudolska, M.; Kalytchuk, S.; Nachtigallova, D.; Rogach, A. L.; Otyepka, M.; Zboril, R. Graphitic Nitrogen Triggers Red Fluorescence in Carbon Dots. *ACS Nano* **2017**, *11*, 12402−12410.

(17) Shao, M.; Yu, Q.; Jing, N.; Cheng, Y.; Wang, D.; Wang, Y. D.; Xu, J. H. Continuous Synthesis of Carbon Dots with Full Spectrum Fluorescence and the Mechanism of Their Multiple Color Emission. *Lab Chip* **2019**, *19*, 3974−3978.

(18) Abdelsalam, H.; Elhaes, H.; Ibrahim, M. A. Tuning Electronic Properties in Graphene Quantum Dots by Chemical Functionalization: Density Functional Theory Calculations. *Chem. Phys. Lett.* **2018**, *695*, 138−148.

(19) Fu, M.; Ehrat, F.; Wang, Y.; Milowska, K. Z.; Reckmeier, C.; Rogach, A. L.; Stolarczyk, J. K.; Urban, A. S.; Feldmann, J. Carbon Dots: A Unique Fluorescent Cocktail of Polycyclic Aromatic Hydrocarbons. *Nano Lett.* **2015**, *15*, 6030−6035.

(20) Kundelev, E. V.; Tepliakov, N. V.; Leonov, M. Y.; Maslov, V. G.; Baranov, A. V.; Fedorov, A. V.; Rukhlenko, I. D.; Rogach, A. L. Amino Functionalization of Carbon Dots Leads to Red Emission Enhancement. *J. Phys. Chem. Lett.* **2019**, *10*, 5111−5116.

(21) Xiong, Y.; Schneider, J.; Ushakova, E. v.; Rogach, A. L. Influence of Molecular Fluorophores on the Research Field of Chemically Synthesized Carbon Dots. *Nano Today* **2018**, *23*, 124−139.

(22) Shi, L.; Yang, J. H.; Zeng, H. B.; Chen, Y. M.; Yang, S. C.; Wu, C.; Zeng, H.; Yoshihito, O.; Zhang, Q. Carbon Dots with High Fluorescence Quantum Yield: The Fluorescence Originates from Organic Fluorophores. *Nanoscale* **2016**, *8*, 14374−14378.

(23) Shamsipur, M.; Barati, A.; Taherpour, A. A.; Jamshidi, M. Resolving the Multiple Emission Centers in Carbon Dots: From Fluorophore Molecular States to Aromatic Domain States and Carbon-Core States. *J. Phys. Chem. Lett.* **2018**, *9*, 4189−4198.

(24) Schneider, J.; Reckmeier, C. J.; Xiong, Y.; von Seckendorff, M.; Susha, A. S.; Kasak, P.; Rogach, A. L. Molecular Fluorescence in Citric Acid-Based Carbon Dots. *J. Phys. Chem. C* **2017**, *121*, 2014−2022.

(25) Song, Y.; Zhu, S.; Zhang, S.; Fu, Y.; Wang, L.; Zhao, X.; Yang, B. Investigation from Chemical Structure to Photoluminescent Mechanism: A Type of Carbon Dots from the Pyrolysis of Citric Acid and an Amine. *J. Mater. Chem. C* **2015**, *3*, 5976−5984.

(26) Xia, C.; Zhu, S.; Feng, T.; Yang, M.; Yang, B. Evolution and Synthesis of Carbon Dots: From Carbon Dots to Carbonized Polymer Dots. *Adv. Sci.* **2019**, *6*, 1901316.

(27) Shi, L.; Yang, J. H.; Zeng, H. B.; Chen, Y. M.; Yang, S. C.; Wu, C.; Zeng, H.; Yoshihito, O.; Zhang, Q. Carbon Dots with High Fluorescence Quantum Yield: The Fluorescence Originates from Organic Fluorophores. *Nanoscale* **2016**, *8*, 14374−14378.

(28) Siddique, F.; Langer, M.; Paloncýová, M.; Medved', M.; Otyepka, M.; Nachtigallová, D.; Lischka, H.; Aquino, A. J. A. Conformational Behavior and Optical Properties of a Fluorophore Dimer as a Model of Luminescent Centers in Carbon Dots. *J. Phys. Chem. C* **2020**, *124*, 14327−14337.

(29) Langer, M.; Hrivnák, T.; Medved', M.; Otyepka, M. Contribution of the Molecular Fluorophore IPCA to Excitation-Independent Photoluminescence of Carbon Dots. *J. Phys. Chem. C* **2021**, *125*, 12140−12148.

(30) Kundelev, E. V.; Tepliakov, N. V.; Leonov, M. Y.; Maslov, V. G.; Baranov, A. V.; Fedorov, A. V.; Rukhlenko, I. D.; Rogach, A. L. Toward Bright Red-Emissive Carbon Dots through Controlling Interaction among Surface Emission Centers. *J. Phys. Chem. Lett.* **2020**, *11*, 8121−8127.

(31) Cappai, A.; Melis, C.; Stagi, L.; Ricci, P. C.; Mocci, F.; Carbonaro, C. M. Insight into the Molecular Model in Carbon Dots through Experimental and Theoretical Analysis of Citrazinic Acid in Aqueous Solution. *J. Phys. Chem. C* **2021**, *125*, 4836−4845.

(32) Becke, A. D. Density-functional Thermochemistry. III. The Role of Exact Exchange. *J. Chem. Phys.* **1993**, *98*, 5648−5652.

(33) Caldeweyher, E.; Ehlert, S.; Hansen, A.; Neugebauer, H.; Spicher, S.; Bannwarth, C.; Grimme, S. A Generally Applicable Atomic-Charge Dependent London Dispersion Correction. *J. Chem. Phys.* **2019**, *150*, 154122.

(34) Van Lenthe, E.; Baerends, E. J. Optimized Slater-type Basis Sets for the Elements 1−118. *J. Comput. Chem.* **2003**, *24*, 1142−1156.

(35) Pye, C. C.; Ziegler, T. An Implementation of the Conductor-like Screening Model of Solvation within the Amsterdam Density Functional Package. *Theor. Chem. Acc.* **1999**, *101*, 396−408.

(36) te Velde, G.; Bickelhaupt, F. M.; Baerends, E. J.; Fonseca Guerra, C.; van Gisbergen, S. J. A.; Snijders, J. G.; Ziegler, T. Chemistry with ADF. *J. Comput. Chem.* **2001**, *22*, 931−967.

(37) Baerends, E. J.; Ziegler, T.; Atkins, A. J.; Autschbach, J.; Bashford, D.; Baseggio, O.; Brces, A.; Bickelhaupt, F. M.; Bo, C.; Boerritger, P. M.; et al.*ADF2019*; SCM; Theoretical Chemistry, Vrije Universiteit: Amsterdam, the Netherlands, https://www.scm.com.

(38) Ehrat, F.; Bhattacharyya, S.; Schneider, J.; Lóf, A.; Wyrwich, R.; Rogach, A. L.; Stolarczyk, J. K.; Urban, A. S.; Feldmann, J. Tracking the Source of Carbon Dot Photoluminescence: Aromatic Domains versus Molecular Fluorophores. *Nano Lett.* **2017**, *17*, 7710−7716.

(39) Krysmann, M. J.; Kelarakis, A.; Dallas, P.; Giannelis, E. P. Formation Mechanism of Carbogenic Nanoparticles with Dual Photoluminescence Emission. *J. Am. Chem. Soc.* **2012**, *134*, 747−750.

https://doi.org/10.1021/acs.jpcc.2c05926
J. Phys. Chem. C 2022, 126, 18170−18176